

Magnetic Solid-Phase Microextraction for Lead Detection in Aqueous Samples Using Magnetite Nanoparticles

Carolina A. S. Silva,^a Raphael L. S. e Silva,^b Alberthmeiry T. de Figueiredo^a and Vanessa N. Alves^{✉*,a}

^aUnidade Acadêmica Especial de Química, Universidade Federal de Goiás, 75704-020 Catalão-GO, Brazil

^bInstituto de Química, Universidade Federal de Goiás, 74690-900 Goiânia-GO, Brazil

A magnetic solid-phase microextraction procedure was developed to detect lead in aqueous samples by flame atomic absorption spectrometry (FAAS). Fe₃O₄ nanoparticles were synthesized by coprecipitation and the crystalline phase was confirmed by X-ray diffraction. The point of zero charge (PZC) indicated that the oxide surface was negatively charged at pH levels above 9.4. pH 9.0 is the best for adsorption and the influence of stirring time and adsorbent mass were analyzed and set at 4 min and 3.0 mg, respectively. The best desorption conditions were obtained for 500 µL of 0.5 mol L⁻¹ HNO₃ as eluant. The limit of quantification (LOQ) and relative standard deviation (RSD) were 16.48 µg L⁻¹ and 0.25%, respectively. The linear range was found to be 16.48-500 µg L⁻¹. The accuracy was evaluated by recovery tests in mineral water, micellar water and aqueous makeup remover samples, showing values in the range of 95.94 to 118%.

Keywords: magnetite, MSPE, lead

Introduction

Humans come into contact with a variety of metal ions in their daily lives, be it in air, water, industrialized products (cosmetics, toiletries, medicines, tattoo dyes, etc.) or in food (from fertilizers, packaging, pesticides, etc.), and this contact is often unavoidable.¹ Lead is the type of metal ion that causes the greatest concern because it is highly toxic and widely used. Lead poisoning causes harmful effects to the central nervous system, blood, heart and kidneys.²

An important technique for trace lead determination in different types of samples, especially in aqueous samples, is flame atomic absorption spectrometry (FAAS), which is simpler and cheaper than other methods.³ Even with the high sensitivity of atomic spectroscopy techniques, a step of the analyte enrichment may be required depending on the type matrix. The use of solid-phase extraction (SPE) techniques has been frequently proposed for this purpose.⁴

Oliveira *et al.*⁵ developed an SPE method for the preconcentration of lead in chicken feed. The procedure involves Pb^{II} adsorption in a column packed with *Moringa oleifera* husks. The limit of detection (LOD)

found was 1.66 µg L⁻¹ and the precision, based on calculated repeatability, was below 1.3%.

In addition to bioadsorbents, highly porous materials with high surface area have been used as adsorbents in SPE techniques. In this context, among the available adsorbents, nanostructured materials present good ability to adsorb toxic metallic ions and organic compounds in different types of samples. Thus, metallic oxides are widely applied in the adsorption of metallic ions in biological and environmental samples.⁶

Magnetic oxides such as magnetite (Fe₃O₄) have received special attention in recent years because of their good adsorption capacity and promising potential for use in different fields of application. Thanks to their adsorptive potential and strong magnetic properties, these oxides are widely used to decontaminate water by removing metal ions, using a combination of adsorption and magnetic separation techniques.^{7,8}

Magnetic solid-phase extraction (MSPE) is a technique that uses magnetic oxides as adsorbents. In this technique, magnetic particles (MPs) are added to the sample solution and the analyte is adsorbed onto the surface of the particles. The MPs are separated from the aqueous solution by an external magnetic force, and the analyte is easily desorbed

*e-mail: vanessanalves@gmail.com

by the eluant.⁹ As in classical SPE, the mechanisms by which the analyte is extracted involve interactions between analyte and functional groups or ions present on the MPs surface, such as hydrogen bonding, ionic, dipole-dipole, dipole-induced dipole and dispersion forces.¹⁰

Suleiman *et al.*¹¹ developed a method to separate and preconcentrate Cr, Cu and Pb traces in environmental samples by MSPE, using bismuthiol II immobilized magnetic nanoparticles. The method is characterized by its high enrichment factor, rapid separation and low LOD, and was successfully applied in river and lake water samples.

Behbahani *et al.*¹² designed and utilized a nanogel composed of Fe₃O₄, silica and poly(4-vinylpyridine) as an adsorbent for the simultaneous separation of ultra-trace amounts of cadmium, lead, copper and nickel ions. Mehdiinia *et al.*¹³ developed a magnetic nanoadsorbent consisting of magnetite nanoparticles coated first with titanium dioxide and then with polypyrrole for MSPE of Pb^{II} trace.

Several studies found in the literature report the use of iron oxide nanoparticles in the development of analytical methodologies. However, most of the works used functionalized materials or that have undergone some previous treatment.

Thus, this study focused on the evaluation of the magnetite obtained by the coprecipitation method in the lead adsorption for the development of an MSPE methodology. The methodology developed will be applied in the lead determination in aqueous samples by FAAS. Since the magnetite nanoparticles used as adsorbent do not have any type of functionalization, the simplicity and low cost of synthesis are evidenced. Thus, the developed method obeys the current principles of green analytical chemistry.

Experimental

Instrumentation

Lead was detected using a Varian SpectrAA 220 FAAS (Mulgrave, Australia) equipped with a hollow cathode lamp and a deuterium lamp for background correction. The device was operated as recommended by the manufacturer. The pH of the samples and the working solutions was adjusted using a Gehaka PG1800 pHmeter (São Paulo, Brazil).

The solutions used in the extraction and elution steps were stirred in an XH-D vortex mixer (Global Trade Technology Co. Ltd., São Paulo, Brazil).

Reagent solutions and samples

The working solutions were prepared with water deionized in a Gehaka water purification system (São Paulo, Brazil). The reagents were of analytical grade. Before use, the laboratory glassware was left overnight in an aqueous solution of 10% (v/v) nitric acid and then rinsed with deionized water.

Working solutions of lead were prepared daily by diluting a 1000 mg L⁻¹ standard lead solution (Carlo Erba, Val de Reuil, France). The nitric acid solution used as eluant was prepared by diluting concentrated nitric acid obtained from Merck (Darmstadt, Germany) in water.

Synthesis of magnetite nanoparticles

Magnetite nanoparticles were obtained by the coprecipitation of Fe³⁺ (FeCl₃·6H₂O) and Fe²⁺ (FeSO₄·7H₂O) (Synth, São Paulo, Brazil) salts (molar ratio of 2:1), using an adapted version of a procedure described by Silva *et al.*¹⁴ The overall reaction can be written as equation 1:



Lastly, the material obtained was oven-dried at 60 °C for 24 h.¹⁴

Characterization of magnetite particles

The crystal structure and crystallinity of the magnetite were analyzed by X-ray diffraction (XRD) (CuKα radiation) in the θ-2θ scan mode (θ is the diffraction angle), using a Shimadzu XRD 6100 diffractometer (Kyoto, Japan). The data were collected in fixed-time mode, from 20 to 80° in the 2θ range, using a divergence slit of 0.5°, a receiving slit of 0.3 mm, and a step size of 0.02°. The surface chemical bonds of the magnetite before and after the extraction process were detected by Fourier transform infrared spectroscopy (FTIR; Shimadzu IRPrestige-21, Tokyo, Japan). The powder samples were mixed with KBr in a 1:100 (m/v) ratio to produce tablets. The spectral range varied from 4000 to 400 cm⁻¹, with 28 scans and 4 cm⁻¹ resolution.

Magnetic solid-phase microextraction method

Aliquots of 5.0 mL of sample containing 1 mg L⁻¹ Pb^{II} under controlled pH (9.0) were poured into polyethylene flasks. Then, 3.0 mg of magnetite nanoparticles were added to the flasks and stirred in a vortex mixer for 4.0 min. The Pb^{II} ions were adsorbed on the adsorbent surface and the

magnetic nanoparticles containing adsorbed ions were separated with a magnet. The supernatant was discarded. The Pb^{II} ions adsorbed on magnetic nanoparticles were eluted using $0.5 \text{ mol L}^{-1} \text{ HNO}_3$ by stirring in a vortex mixer for 2 min. After the elution step, the nanoparticles were collected using a magnet and the supernatant was analyzed by FAAS.

Optimization of the extraction and elution steps

The effect of pH on the adsorption of Pb^{II} by magnetite nanoparticles was investigated at pH levels of 1, 3, 5, 7, 9 and 12. The lead solution used in the optimization experiments was prepared in the concentration of 1 mg L^{-1} . The pH was adjusted by adding $0.1 \text{ mol L}^{-1} \text{ HNO}_3$ or NH_4OH . In this experiment, the variables of adsorbent mass and stirring time were fixed at 6.3 mg and 30 min, respectively. After this time, the magnetite nanoparticles containing adsorbed Pb^{II} were collected with a magnet and the supernatant was analyzed by FAAS.

After selecting the best pH level for Pb^{II} adsorption, the extraction variables were optimized using a univariate approach. The selected parameters were adsorbent mass and stirring time. In this experiment, the magnetite nanoparticles containing adsorbed Pb^{II} were collected with a magnet and the supernatant was analyzed by FAAS.

To evaluate the influence of the magnetite mass on the extraction process, mass aliquots of 3.0, 6.0, 12.0, 25.0 and 50.0 mg were investigated. These aliquots were stirred for 30 min with solutions of Pb^{II} (1 mg L^{-1}) and pH 9.0. Then, the stirring time was studied in the range of 1 to 10 min.

After optimizing the adsorption process, the desorption parameters were evaluated: eluant (HNO_3) concentrations of 0.1, 0.5, 1.0 and 2.0 mol L^{-1} and elution times of 2, 4, 8, 10 and 12 min. For this evaluation, the magnetite containing adsorbed Pb^{II} was put into contact with the eluant at the above-cited concentrations. The magnetite was separated magnetically, and the eluate analyzed by FAAS.

Study of interfering ions

The effect of Fe^{II} , Cu^{II} , K^{I} , Zn^{II} , Ca^{II} , Na^{I} , Mg^{II} , Co^{II} , Cd^{II} and Cr^{III} was evaluated to determine the potential of these ions to interfere in the adsorption of 1.0 mg L^{-1} of lead solution by the preconcentration method.

The influence of potentially interfering ions was determined by comparing the analytical signals of a solution containing only Pb^{II} and a solution containing Pb^{II} ions together with the potentially interfering ions. These solutions were preconcentrated and the interference factor ($\text{IF} = A' / A$) was calculated. A' is the analytical signal

for the solution containing the analyte in the presence of possible interferents, and A is the analytical signal for the solution containing Pb^{II} in the absence of possible interferents. Species A was considered an interferent whenever the difference between the analytical signal for the solution containing only Pb^{II} ions and the solution that also contained possible interfering ions was higher than 10%.⁵

Results and Discussion

Characterization of magnetite nanoparticles

Since the synthesized material is completely magnetic, after preparation, the magnetite was completely removed from solution by magnetic decanting.

The method of synthesis and the concentration of reagents determine the chemical and physical properties of the synthesized nanoparticles, affecting their degree of crystallinity.¹⁵ Figure 1 depicts the XRD pattern of magnetite synthesized by coprecipitation.

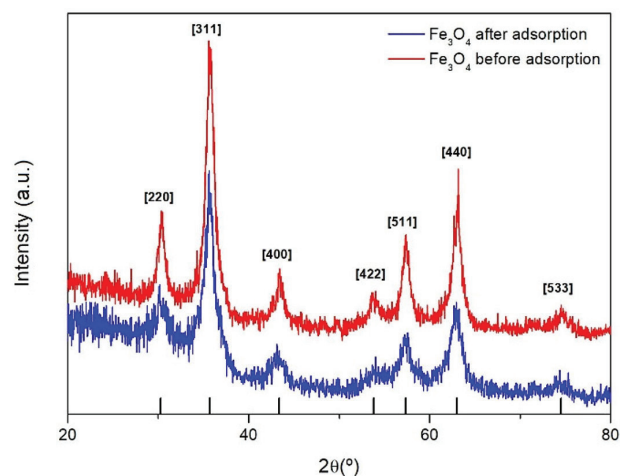


Figure 1. Fe_3O_4 diffratograms before and after adsorption.

Figure 1 depicts the profile of the magnetite nanoparticles used as adsorbent before and after the extraction of lead ions. After the Fe_3O_4 peaks were indexed, the cubic structure of magnetite was identified and found to be in good agreement with the Joint Committee on Powder Diffraction Standards (JCPDS) card No. 089-096. In addition, a comparison of the diffraction patterns and the crystallographic form of Fe_3O_4 revealed the absence of diffraction peaks for other phases, indicating that the synthesized material contained only the phase corresponding to the inverse spinel structure of the magnetite and that, after the lead was extracted, this structure did not undergo appreciable structural modifications.

The mean crystallite size of the samples was calculated based on the peak width using the Debye-Scherrer equation, as: $D_{hkl} = \frac{0.89\lambda}{\beta \cos\theta}$, where D_{hkl} is the crystallite size, λ is the X-ray wavelength used (ca. 1.54056 Å), θ is the diffraction angle, and β is the full width at half maximum (FWHM, in radians) of the diffraction peak (311). The calculated crystallite size was corrected using instrumental broadening and was found to be 7.95 nm. Thus, the synthesized magnetite was nano-sized.

Adsorption is essentially a surface phenomenon, and any nano-sized materials have far larger surface areas than similar masses of larger scale materials. Thus, a larger amount of the magnetite can come into contact with the surrounding lead analyte, thereby increasing the adsorption.

Figure 2 shows the FTIR spectra of the magnetite before and after the adsorption process. Note the characteristic vibrations of the Fe–O bonds of the magnetite at around 624 to 425 cm^{-1} . The band at 1622 cm^{-1} is due to water molecules adsorbed on the magnetite surface.^{16,17} The characteristic O–H bending vibrations are indicated by the bands at 3405 cm^{-1} . After adsorption, there is a slight shift in the band centered at 567 cm^{-1} , corresponding to the Fe–O bonds, which shifts to 574 cm^{-1} , indicating the formation of Fe–O–Pb on the magnetite surface.^{7,17}

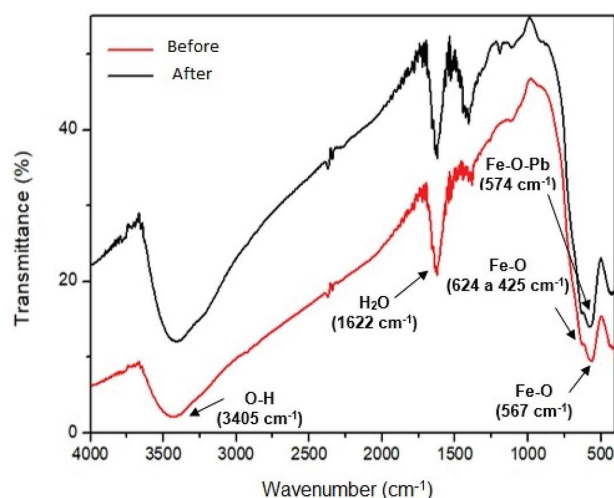


Figure 2. FTIR analysis of magnetite nanoparticles before and after adsorption.

Optimization of the extraction and elution steps

In the last few years, magnetite has been used in several scientific fields for a wide range of applications. Its adsorption potential has been evaluated against numerous organic and inorganic compounds. Thus, the influence of pH on Pb^{2+} adsorption by magnetite particles was evaluated, and this behavior is illustrated in Figure 3.

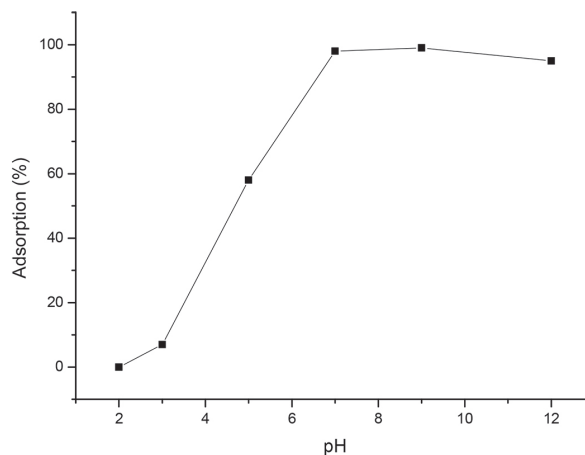


Figure 3. pH influence on lead adsorption.

High lead adsorption occurs between pH levels of 7.0 and 9.0. This behavior is probably due to the fact that, in aqueous media, the surface of magnetite is covered with FeOH groups. These groups can protonate or deprotonate to generate surface loads (FeOH_2^+ or FeO^-), which vary according to pH levels below or above the pH_{PZC} (pH of the point of zero charge (PZC)), respectively. The pH_{PZC} of this material is 9.4, indicating that below this value, the surface of the magnetite will contain groups with mostly positive loads (FeOH_2^+), although the coexistence of a small number of groups with negative loads (FeO^-) is possible.⁷ At pH levels between 7.0 and 9.0, lead has different species (Pb^{2+} , $\text{Pb}(\text{OH})^+$ and $\text{Pb}(\text{OH})_2$). These species are electrostatically attracted by the surface loads of the coexisting magnetite species. This attraction causes a considerable increase in the adsorption of the lead species in these conditions.

The evaluation of the maximum adsorptive capacity of magnetite nanoparticles was evaluated by the construction of adsorption isotherms. The non-linear adjustment to the Langmuir, Freundlich and Sips models was evaluated.

The Sips model was the one that best represented the adsorption system; values for X^2 (non-linear chi-square, 2.5847) and R^2 (coefficient of determination, 0.9855), were observed for this model. The heterogeneity index ($nS = 0.4072$) indicates that the system presents a mixed adsorption mechanism that at a given moment takes the form of Freundlich isotherm and subsequently takes the form of the Langmuir isotherm.¹⁸ The Q_{max} value (maximum adsorption capacity, 31.68 mg g^{-1}) indicates a good performance of the adsorbent.

In SPE procedures, the dose of adsorbent plays an important role in the adsorption of analytes.¹⁷ To determine the effects of adsorbent dose on the quantitative retention of lead, varying amounts of magnetite, ranging from 3.0 to 50.0 mg, were added to the lead solutions, and the MSPE method developed here was applied. Altering the amount

of adsorbent mass does not cause significant changes in the adsorption efficiency of Pb^{II} ions by magnetite. This means the process can be carried out using the smallest mass concentration evaluated in this study, i.e., 3.0 mg.

To ensure high adsorption efficiency and speed in the extraction process, the adsorption of Pb^{II} by magnetite was evaluated within a range of 1 to 10 min. It was found that the amount of ions Pb^{II} adsorbed by magnetite in a time frame of 1 to 4 min increased considerably, thereafter remaining constant up to 10 min. Therefore, to ensure the analytical frequency, a duration of 4 min was established as the optimal equilibrium time.

To determine the kinetic parameters of the adsorption mechanism of Pb^{II} by magnetite, the experimental data was adjusted to the kinetic models of pseudo-first order, pseudo-second order and the Avrami fractional model, using the nonlinear method. Table 1 compares the parameters obtained for the three tested models.

Overall, the amounts of metal ion adsorbed *per* unit mass of the adsorbent at time *t* (q_t) values calculated by the models and the q_e values obtained experimentally showed no significant differences. However, the pseudo-first order model provided the best values of both R² and X², indicating that the adsorption rate in this process is proportional to the number of active sites available in the adsorbent material.

After determining the best conditions for Pb^{II} adsorption, the desorption parameters were evaluated in order to identify the best conditions for the removal of Pb^{II} adsorbed on the magnetite surface.

As shown in Figure 3, the adsorption process is highly dependent on the pH, the adsorbed lead ions can be eluted from the magnetite surface with the decrease of the pH of the solution. Thus, nitric acid solutions were used as eluant.

The addition of acidic solutions alters the pH of the medium, leading to a change in the surface load of the adsorbent. Considering that the magnetite has a PZC of

9.4, its surface will be more positively charged and will repel lead ions present, favoring the desorption process.

The evaluation of desorption time and eluant concentrations used in the desorption process indicated that the best result was achieved with 2 min of desorption and 0.5 mol L⁻¹ of nitric acid.

Study of interfering ions

It is well known that the efficiency of a preconcentration can be affected by the composition of the sample matrix. Therefore, the effect of some potentially interfering ions was evaluated. Our findings suggest that Cd^{II} (IF = 0.86) and Fe^{III} (IF = 0.67) ions favor a decrease in the analytical signal, indicating their negative interference in the process. However, the other ions (Cu^{II}, K^I, Zn^{II}, Ca^{II}, Na^I, Mg^{II}, Co^{II} and Cr^{III}) interfered positively, causing an increase in the analytical signal. This interference can usually be attributed to several factors, such as molecular mass, electronegativity and ionic radius.¹⁹ Another possibility is that this interference may occur not only in the solid phase of the adsorbent but also in the flame atomization step.²⁰

Analytical performance of the method

Some analytical characteristics of the proposed method were evaluated after the system was optimized. The LOD was estimated to be three times the standard deviation of ten independent measurements of a blank sample divided by the slope of the calibration curve, and this value was 5.44 µg L⁻¹. The linear range was 16.48 to 500 µg L⁻¹, and the correlation coefficient was 0.999. The repeatability of the proposed method was assessed by performing ten consecutive preconcentration steps at a concentration of 500 µg L⁻¹, whose results were expressed in terms of the relative standard deviation (RSD), which was equal to 0.25%.

Table 1. Kinetic parameters for Pb^{II} adsorption using Fe₃O₄ as adsorbent

Pseudo-first order					
K_1 / min^{-1}	$q_e \text{ calc.} / (\text{mg g}^{-1})$	$q_e \text{ exp.} / (\text{mg g}^{-1})$	R ²	X ²	
0.631	1.6888	1.6666	0.9299	0.0058	
Pseudo-second order					
K_2 / min^{-1}	$h_0 / (\text{mg g}^{-1} \text{ min}^{-1})$	$q_e \text{ calc.} / (\text{mg g}^{-1})$	$q_e \text{ exp.} / (\text{mg g}^{-1})$	R ²	X ²
0.4252	1.61	1.9496	1.6666	0.9059	0.0078
Avrami					
K_{AV} / min^{-1}	n_{AV}	$q_e \text{ calc.} / (\text{mg g}^{-1})$	$q_e \text{ exp.} / (\text{mg g}^{-1})$	R ²	X ²
0.5362	0.8195	1.7029	1.6666	0.9247	0.0062

K_1 : pseudo-first order rate constant of the sorption process; $q_e \text{ calc.}$ and $q_e \text{ exp.}$: calculated and experimental amounts of metal ion adsorbed *per* unit mass of the adsorbent at time *t*, respectively; R²: coefficient of determination; X²: non-linear chi-square; K_2 : pseudo-second order rate constant of the sorption process; h_0 : initial adsorption rate; K_{AV} : constant kinetics of Avrami; n_{AV} : fractional order of the reaction related to the adsorption mechanism.

In this work, the preconcentration factor was calculated according to other studies,⁵ as the ratio between the sensitivity of a calibration curve submitted to the preconcentration procedure and a calibration curve without the preconcentration. The sensitivity of the calibration curve submitted to the preconcentration was 0.0027, while for the curve without preconcentration, the sensitivity obtained was 2×10^{-5} . Thus, the preconcentration factor obtained was 135.

According to the Conselho Nacional do Meio Ambiente (CONAMA)²¹ and the Environmental Protection Agency (EPA),²² the maximum allowable value for lead ions in effluents should not exceed 0.5 mg L^{-1} , while for drinking water it is 0.05 mg L^{-1} .

Compared to other extraction and preconcentration methods such as those developed by Baghban *et al.*²³ and Carasek,²⁴ who presented LOD values of 100 and $10 \text{ } \mu\text{g L}^{-1}$, respectively, the proposed methodology is efficient.

The proposed method was applied to quantify lead in aqueous samples. Pb^{II} was not detected in these samples, so the samples were spiked with Pb^{II} to reach a final concentration of $25 \text{ } \mu\text{g L}^{-1}$. As can be seen in Table 2, recovery rates of 95.54 to 118% were achieved.

Table 2. Relative recovery rates of the samples subjected to the proposed method

Sample	$\text{Pb}^{\text{II}} / (\mu\text{g L}^{-1})$		Recovery / %
	Added	Found	
Micellar water 1	25.00	25.00	100.01
Micellar water 2	25.00	25.01	100.05
Micellar water 3	25.00	25.16	100.65
Makeup remover	25.00	24.07	96.29
Mineral water 1	25.00	29.50	188.00
Mineral water 2	25.00	27.27	109.09
Mineral water 3	25.00	23.98	95.54

The accuracy of the method was evaluated by analyzing a certified river water sample (APS-1071) with a certified lead concentration of $100.00 \pm 0.5 \text{ mg L}^{-1}$. The reference material was subjected to MSPE, which resulted in $100.42 \pm 0.12 \text{ mg L}^{-1}$. This is in good agreement with the certified values, confirming the reliability of the proposed method.

Conclusions

In this study, magnetic Fe_3O_4 nanopowder was prepared by a chemical coprecipitation method. The synthesized particles had a diameter of 7.95 nm. The characterization

results indicated that the material did not undergo structural changes in response to the adsorption of lead. Therefore, the MPs were used as a promising sorbent for the MSPE of trace amounts of lead in samples of mineral water, micellar water and makeup remover by FAAS. Magnetite provided excellent magnetic separation and dispersibility. The stability test, which consisted of successive cycles of separation / elution using $0.5 \text{ mol L}^{-1} \text{ HNO}_3$ as eluant, indicated that the same batch of nanoparticles can be subjected to up to 10 cycles. The method provides good performance characteristics when compared to other FAAS methods described in the literature, and can be considered a simple and inexpensive method for the detection of lead in cosmetics and other aqueous media.

Acknowledgments

The present work was carried out with the support of the Coordenação de Aperfeiçoamento de Pessoal de Nível Superior (CAPES) - Brazil - Financing code 001. The authors gratefully acknowledge the Brazilian research funding agencies CNPq (Conselho Nacional de Desenvolvimento Científico e Tecnológico) and FAPEG (Fundação de Amparo à Pesquisa do Estado de Goiás) for their financial support of this work.

References

- Marinovich, M.; Boraso, M. S.; Testai, E.; Galli, C. L.; *Regul. Toxicol. Pharmacol.* **2014**, *69*, 416.
- Kleinubing, S. J.; Silva, M. G. C.; *Cienc. Eng.* **2006**, *2*, 83.
- Yilmaz, E.; Soylak, M.; *Talanta* **2018**, *15*, 152.
- Alves, V. N.; Neri, T. S.; Borges, S. S. O.; Carvalho, D. C.; Coelho, N. M. M.; *Ecol. Eng.* **2017**, *106*, 431.
- Oliveira, J. A. N.; Siqueira, L. M. C.; de Sousa Neto, J. A.; Coelho, N. M. M.; Alves, V. N.; *Microchem. J.* **2017**, *133*, 4327.
- Mortavazi, K.; Ghaed, M.; Roosta, M.; Montazerzohori, M. N.; *Indian J. Sci. Technol.* **2012**, *5*, 1983.
- Rajput, S.; Pittman, C. U.; Mohan, D.; *J. Colloid Interface Sci.* **2016**, *48*, 334.
- Shirani, M.; Habibollahi, S.; Akbari, A.; *Food Chem.* **2019**, *30*, 304.
- Arteaga, A. K.; Rodriguez, A. J.; Barrado, E.; *Anal. Chim. Acta* **2010**, *64*, 1657.
- Zygler, A.; Wasik, A.; Namiéńnik, J.; *Talanta* **2010**, *82*, 1742.
- Suleiman, J. S.; Hu, B.; Peng, H.; Huang, C.; *Talanta* **2009**, *77*, 1579.
- Behbahani, M.; Bide, Y.; Bagheri, S.; Salariam, M.; Omid, F.; Nabid, M. R.; *Microchim. Acta* **2018**, *183*, 111.
- Mehdini, A.; Shoormeij, Z.; Jabbari, A.; *Microchim. Acta* **2017**, *184*, 1529.

14. Silva, R. L. S.; Figueiredo, A. T.; Barrado, C. M.; Sousa, M. H.; *Mater. Res.* **2017**, *20*, 1317.
15. Lu, A.; Salabas, E. L.; Schuth, F.; *Angew. Chem.* **2007**, *46*, 122.
16. Kumari, M.; Pittman Jr., C. U.; Mohan, D.; *J. Colloid Interface Sci.* **2015**, *442*, 120.
17. Feist, B.; *Food Chem.* **2016**, *209*, 37.
18. Nagy, B.; Mânzatu, C.; Maicanranu, A.; Indolean, C.; Lucian, B.; Majdik, C.; *Arabian J. Chem.* **2017**, *10*, 569.
19. Nassar, N. N.; *J. Hazard. Mater.* **2010**, *184*, 538.
20. Tarley, C. R. T.; Ferreira, S. L. C.; Arruda, M. A. Z.; *Microchem. J.* **2004**, *77*, 163.
21. Conselho Nacional do Meio Ambiente (CONAMA); *Resolução CONAMA No. 430 de 13/05/2011*. Available at <https://www.legisweb.com.br/legislacao/?id=114770>, accessed in May 2019.
22. <https://www.usa.gov/federal-agencies/environmental-protection-agency>, accessed in January 2019.
23. Baghban, N.; Yilmaz, E.; Soylak, M.; *J. Mol. Liq.* **2010**, *34*, 260.
24. Carasek, E.; *Quim. Nova* **2002**, *25*, 748.

Submitted: February 7, 2019

Published online: June 7, 2019

